Unzipping an adsorbed polymer in a dirty or random environment

Rajeev Kapri and Somendra M. Bhattacharjee*
Institute of Physics, Bhubaneswar 751005, India
(Received 12 May 2005; published 2 November 2005)

The phase diagram of unzipping of an adsorbed directed polymer in two dimensions in a random medium has been determined. Both the hard-wall and the soft-wall cases are considered. Exact solutions for the pure problem with different affinities on the two sides are given. The results obtained by the numerical procedure adopted here are shown to agree with the exact results for the pure case. The characteristic exponents for unzipping for the random problem are different from the pure case. The distribution functions for the unzipped length, first bubble, and the spacer are determined.

DOI: 10.1103/PhysRevE.72.051803 PACS number(s): 82.35.Gh, 64.60.Fr, 82.37.Rs

I. INTRODUCTION

The study of polymer adsorption on a surface is important because of many applications such as in lubrication, adhesion, surface protection, coating of surfaces, wetting, vortex lines, and biology. Of particular interest is the adsorption-desorption transition of a polymer, similar to the denaturation transition of a double stranded DNA molecule. The adsorbed phase, dominated by the attraction with the wall, wins at low temperatures whereas at high temperatures the desorbed phase prevails. Although the temperature driven adsorption-desorption transition dates back to the 1960s [1–5], the advent of micromanipulation techniques such as optical tweezers, atomic force microscopy (AFM), etc. [6,7] regenerated interest in it because of the possibility of exploring single molecules especially under an external force.

The existence of a force induced unzipping transition was established theoretically for DNA type double stranded molecules in Ref. [8]. Many aspects of the unzipping transition have now been elucidated [9–14], including an experimental phase diagram [15]. The basic feature of the unzipping transition is that, at a fixed temperature T, the polymers stay in the bound or localized phase if the magnitude of the pulling force, g, is less than the critical force $g_c(T)$, but they can be unbound or unzipped if the pulling force exceeds the critical force. Moreover, the transition is described by a set of characteristic exponents. Since this transition involves a competition between a binding potential and the stretching by the force, such an unzipping transition is also possible for an adsorbed polymer [16,17].

Apart from thermal fluctuations and force, disorder (or impurities) in the medium may also induce the adsorption-desorption transition even below the desorption transition temperature. This phenomenon is known as a *depinning transition*. The depinning transition for a directed polymer has been studied in the past because of its importance in understanding fluctuations in domain walls in random magnet, pinning of magnetic flux lines in dirty superconductors having columnar defects, and in particular as a simpler sibling of the more complex polymer adsorption problem [18–20]. In a homogeneous medium, in absence of any attraction with the wall, a polymer behaves like a free chain controlled by entropy. But with quenched impurities, there may be one or more ground state configurations [21]. As a result, a polymer may swell over a free chain to take advantage of the attractive locations in the medium. This swelling effect is pronounced in lower dimensions and would affect the response of the polymer to any applied force. More importantly, because the impurities are quenched (no thermalization allowed), the behavior of a polymer is sample dependent. An averaging over the samples often yields well-behaved thermodynamic quantities but still sample variations may reveal drastic differences from the average behavior. Consequently the unzipping phenomenon in a random medium ("dirty environment") is expected to be different from that in a homogeneous medium because, in the random case, it is not just pulling off from the wall but also pulling away from local pockets of favorable configurations.

In this paper our aim is to study the phase diagram, of a directed polymer which is adsorbed on a wall in a random environment and pulled by a force at one end to unzip it off the wall, keeping the other end fixed. Though the unzipping transition in a pure system is first order, randomness may change the order of the transition. This change will be reflected in the exponents that describe the transition. Therefore, in addition to the overall phase diagram, we would also like to determine the exponents in this paper.

The disorder in the problem can be introduced in several ways as shown in Fig. 1. These possibilities are as follows: (i) The polymer sequence is homogeneous, and the randomness is introduced on the lattice site such that the ground state of the polymer (on the wall) remains unaffected as if it is in a pure environment. In this case the binding from the wall is attractive and constant. (ii) The randomness is introduced in the polymer sequence but the environment is kept pure. The binding from some portion of the wall, depending on the strength of randomness, can be attractive or repulsive. The ground state in this case is sample dependent. (iii) The randomness is put at each lattice point including the wall. For strong enough disorder some sites of the wall may become repulsive. In this case also the ground state is sample dependent. Of these, item (ii) of heterogeneous sequence is of importance because of its similarity with the DNA unzipping problem. In this paper we restrict ourselves to case (iii)

*Electronic address: rajeev@iopb.res.in, somen@iopb.res.in

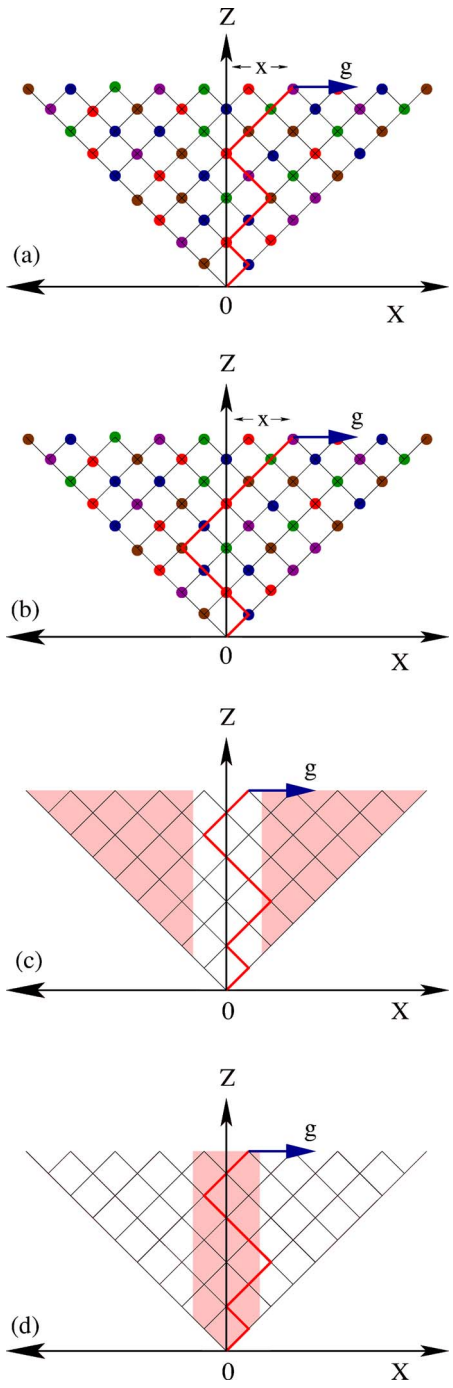

FIG. 1. (Color online) Schematic diagram of a direct polymer in a random medium with an attractive wall. By construction, one direction along the polymer is special. The wandering is in the transverse d direction and therefore it is a $d+1$ dimensional model. Here $d=1$. There is a line at $x=0$ (a wall or an interface) that attracts the polymer. (a) Hard wall: polymer is not allowed in the region $x<0$. (b) Soft wall: polymer is allowed in the whole region. There may be an extra potential $V(>0)$ on one side, say $x<0$. (c) Homopolymer in random medium. There is a unique (sample independent) ground state for this case. (d) Hetropolymer in pure medium. The ground state is sample dependent. In (c) and (d), randomness is in the shaded regions.

only, especially because of the known behavior of a polymer in a random or dirty medium.

The thermodynamic or bulk behavior is described by temperature and one of the two conjugate variables force or distance. This results in two different ensembles, namely the fixed force and the fixed distance ensemble. For the pure case the ensembles are equivalent when the polymer is pulled at the end. But this is not always the case. It is shown recently by Kapri *et al.* [13] in the context of DNA unzipping that the ensembles are not equivalent when the pulling force is applied at any fraction $s\,(0<s<1)$ on the double stranded DNA. In this respect pulling at the end is a special case in which results happened to be ensemble independent. We restrict ourselves to the force at the end case only and again show that the pure phase diagram can be obtained exactly from both the ensembles. However, there are subtle differences and such differences play a significant role in the random case.

Apart from exact solutions for the pure case, our approach involves the use of exact transfer matrix for a polymer on a two-dimensional square lattice. The choice of two dimensions is partly influenced by the known results of strong effect of disorder in lower dimensions. The paper is organized as follows: The model is described in Sec. II. The quantities of interest are also defined here. In Sec. III we discuss the adsorption-desorption transition in absence of randomness. The exact phase diagram and a comparison with exact transfer matrix results can be found here. We also explain the use of finite size scaling to extract the critical value and the exponents from the results of extensibility for finite chains. A general case of the adsorbing wall separating media of two different types is also discussed. Section IV is devoted to the case of a polymer in a random environment. We determine the phase diagram and the changes in the exponents due to randomness. These are based on the results of the transfer matrix for finite chains and are therefore exact for each sample. The statistical error comes only because of averaging over a finite sample size. For the data collapse in finite size scaling analysis, the Bhattacharjee-Seno procedure has been adopted [22].

II. MODEL

We model a polymer by a directed random-walk in a two-dimensional $(d=1+1)$ square lattice directed along the diagonal of the square. There is an attractive wall on the diagonal of the square $(x=0)$ which tends to suppress wandering because the polymer gains an energy $-\epsilon(\epsilon>0)$ each time it is on the wall [23]. Depending on the ensemble one is working with, either a fixed force, g, is applied at the end monomer (*fixed force ensemble*) or the distance, x, of the end monomer from the wall is kept fixed (*fixed distance ensemble*). The other end is always kept anchored. Two types of walls are possible, namely (i) a hard wall if the polymer cannot cross the wall, and (ii) a soft wall if the polymer can cross the wall. For the random case, there is an additional random energy at each lattice point. In a continuum notation, the Hamiltonian may be written as

$$H = \frac{d}{2}K\int_0^N dz\left(\frac{\partial \mathbf{r}}{\partial z}\right)^2 + \int_0^N dz V_w(\mathbf{r}(z)) + \int_0^N dz\ \eta(\mathbf{r}(z),z) - \mathbf{g}\cdot\int_0^N \frac{\partial \mathbf{r}}{\partial z}dz, \tag{1}$$

where $\mathbf{r}(z)$ is the d-dimensional coordinate at monomer index z, $V_w(\mathbf{r})$ is the potential due to the wall, η is the random energy, and $\mathbf{g}$ is the applied force at the end point $z=N$. In this paper we consider a discrete version (Fig. 1) of this model.

A more general case can be considered where the polymer experiences different potentials on the two sides of the wall, as, e.g., may happen for adsorption at the interface of two immiscible liquids with different affinities for the polymers. A hard wall case may then correspond to a solid-liquid interface. The general case is considered in the next section and in detail in Appendix A.

A. Pure case

The partition function for the pure case is obtained by a recursion relation

$$Z_{N+1}(x) = \sum_{j=\pm 1} Z_N(x+j)[1+(e^{\beta\epsilon}-1)\delta_{x,0}], \tag{2}$$

where $Z_N(x)$ is the canonical partition function of the polymer of length N whose Nth monomer is at a distance x from the wall, the zeroth monomer being at $x=0$, and β is the inverse temperature $1/T$ in units of the Boltzmann constant $k_B=1$. The temperature dependence of the partition function has not been shown explicitly. The initial condition for the above recursion relation of the partition function is

$$Z_0(x) = e^{\beta\epsilon}\delta_{x,0}. \tag{3}$$

The noncrossing constraint of the polymer at the hard-wall is taken care of by reassigning

$$Z_j(x) = 0, \quad \forall\ x < 0 \quad \text{(hard-wall)} \tag{4}$$

after each step j.

The canonical partition function with a force, g, acting at one end keeping the other end fixed is then calculated by summing over all the allowed configurations of the walks on the lattice.

$$\mathcal{Z}_N(g) = \sum_x Z_N(x)e^{\beta g x}, \tag{5}$$

where $e^{\beta g x}$ is the Boltzmann weight due to force g. The thermodynamic properties in a given ensemble are obtained from the free energy,

$$F_N(T,x) = -T\ln Z_N(x) \quad \text{(fixed distance)} \tag{6a}$$

$$\mathcal{F}_N(T,g) = -T\ln \mathcal{Z}_N(g) \quad \text{(fixed force)}. \tag{6b}$$

B. Ensembles

For the fixed distance ensemble, the distance, x, of the last (Nth) monomer from the wall is kept fixed. The quantity of interest, the average force required to maintain this distance, is given by

$$\langle g\rangle = \frac{\partial F(T,x)}{\partial x} \quad (k_B=1) \tag{7}$$

and is obtained by the finite difference in free energy $F(x)$ of Eq. (6a) for the lattice problem.

In the fixed force ensemble, the average distance of the last monomer from the wall, $\langle x\rangle$, where a fixed force, g, is applied is the quantity of interest and can be obtained by

$$\langle x\rangle = \frac{\sum_x x Z_N(x)e^{\beta g x}}{\sum_x Z_N(x)e^{\beta g x}}. \tag{8}$$

The finite size effects in fixed distance ensemble are weak which gives the privilege of working with a chain of shorter length and still getting the exact phase boundary. In contrast, the fixed force ensemble exhibits strong finite size effects and finite size scaling has to be used to get the phase boundary.

The response of the polymer is characterized by a susceptibility like quantity to be called *isothermal extensibility* defined as

$$\chi_T = \frac{\partial\langle x\rangle}{\partial g}. \tag{9}$$

This extensibility can be expressed in terms of the position fluctuation in the fixed force ensemble as

$$\chi_T = \frac{1}{k_B T}(\langle x^2\rangle - \langle x\rangle^2). \tag{10}$$

This relation is useful for numerical computation. We determine the isotherms g vs $\langle x\rangle$ or $\langle g\rangle$ vs x (depending on the ensemble).

C. Polymer in a random environment

In the random environment the recursion relation has also the contribution due to the randomness. The recursion relations in the fixed distance and the fixed force ensemble, respectively, read as

$$Z_{N+1}^{\{\alpha\}}(x) = \sum_{j=\pm 1} Z_N^{\{\alpha\}}(x+j)[1+(e^{\beta\epsilon}-1)\delta_{x,0}]\times e^{-\beta\eta(x,N+1)}, \tag{11a}$$

where $\eta(x,N)$ is the random energy at site (x,N), and

$$\mathcal{Z}_N^{\{\alpha\}}(g) = \sum_x e^{\beta g x}Z_N^{\{\alpha\}}(x). \tag{11b}$$

The superscript α in the above equations denotes a particular realization. For every sample, Eqs. (3) and (4) remain valid so that these recursion relations can be used both for soft-wall and hard-wall cases.

The random energies are independently distributed with no spatial correlation (white noise), drawn from a uniform

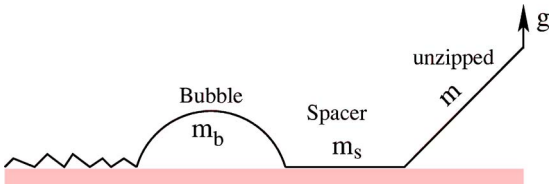

FIG. 2. (Color online) Schematic diagram showing the first bubble of length m_b, spacer of length m_s, and the unzipped segment of length m when a pulling force g is applied at one end of the polymer in the random medium.

deviate of zero mean $\langle \eta(x,\tau)\rangle=0$, width Δ, and

$$[\eta(x,\tau)\eta(x',\tau')]_{\rm dis}=\frac{\Delta^2}{12}\delta(x-x')\delta(\tau-\tau'). \qquad (12)$$

Throughout this paper $[\cdots]_{\rm dis}$ denotes the average over various realizations and $\langle\cdots\rangle$ denotes the thermal averaging.

The thermodynamic quantities with quenched randomness come from the average free energy of the appropriate ensemble, i.e., the average of $F_N^{\{\alpha\}}(x)$ for the fixed distance ensemble, and $\mathcal{F}_N^{\{\alpha\}}(g)$ for the fixed force ensemble.

With $\epsilon=0$, the randomness leads to a swelling of the polymer chain as measured by the transverse size

$$[\langle x_N^2\rangle]_{\rm dis}\sim N^{2\nu}, \qquad (13)$$

where $\nu=2/3$ in two (1+1) dimensions [21]. For a pure system, $\nu=1/2$.

It is apparent that the critical force needed to unzip a polymer has to be sample dependent. Even in a fixed force ensemble, with g at its critical value, the whole chain may not be unzipped in all samples. Important quantities to study are then the unzipped length m measured from the open end to the first contact ("Y-fork"), the length m_s of the completely zipped region after that, to be called a spacer, and then the length m_b of the first bubble. A bubble is defined as an unzipped region separated by two contacts or bound monomers. These are defined in Fig. 2. Apart from the phase diagram obtained by studying the response functions averaged over samples, the distribution functions of the various lengths over samples are determined.

III. EXACT SOLUTION: PURE CASE

A. Phase boundary

The recursion relations, Eqs. (2) and (5), for the pure case, can be analyzed exactly. A more general case where the polymer is adsorbed at the interface of two different types of media (e.g., immiscible liquids with different affinity for the polymer) is considered [16] and a generating function based derivation is given in Appendix A. Also we show how the phase diagram can be obtained from a fixed distance ensemble.

The difference in affinity is modeled by a potential $V>0$ for $x<0$. $V<\infty$ would correspond to two immiscible liquids while the hard-wall $V\to\infty$ corresponds to an interface between a liquid and an impenetrable solid. The homogeneous soft-wall case corresponding to the $V\to 0$ limit. For any $V\neq 0$, there is a temperature driven desorption transition with $T_c\to\infty$ as $V\to 0$. The unzipping transition is given by ($u=e^{-\beta\epsilon}$ and $v=e^{-\beta V}$)

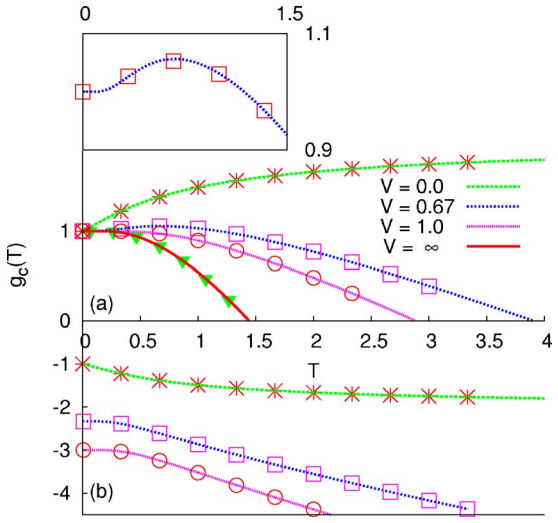

FIG. 3. (Color online) Dimensionless force (g) vs temperature (T) phase diagram for an adsorbed polymer. Each lattice site on one side ($x<0$) of the wall has a repulsive potential of strength $V>0$. Positive g corresponds to the case of pulling the polymer away from the wall on the favorable side while the negative g (note the different scale) is for pulling on the wrong side. The two limiting cases are $V\to 0$ (soft-wall) and $V\to\infty$ (hard-wall). The points are from numerics and the lines are the exact analytical results. Note the reentrance on the positive side for $V=0.67$ (shown in inset).

$$g_c(T)=T\ln\left[\frac{1+v(1-2u)}{u(1-uv)}-1\right], \qquad (14a)$$

or, equivalently,

$$g_c(T)=2T\cosh^{-1}\left[\left\{1-\left(1-\frac{2u(1-vu)}{1+v(1-2u)}\right)^2\right\}^{-1/2}\right]. \qquad (14b)$$

To be noted is the small region at intermediate temperatures where a reentrance can be observed. The details are given in Appendix A.

The unzipping on the wrong side, i.e., with $x<0$ where $V>0$, has a different phase boundary than Eqs. (14a) and (14b) and is given by

$$g_c(T)=-2T\cosh^{-1}\left[\frac{1}{v}\left\{1-\left(1-\frac{2u(1-vu)}{1+v(1-2u)}\right)^2\right\}^{-1/2}\right]. \qquad (15)$$

The phase diagram is not symmetric around $g=0$, except for $V=0$. The critical force need not tend to zero at the transition temperature to unzip on the wrong side. At $T=0$, the critical force for this model is $g_c(0)=-2(V+\epsilon/2)$. More details of the phase diagram for $V\neq 0$ will be discussed elsewhere.

Figure 3 shows the phase diagram for general V, including the soft-wall and the hard-wall cases. The lines are from exact results and the symbols from the numerical analysis

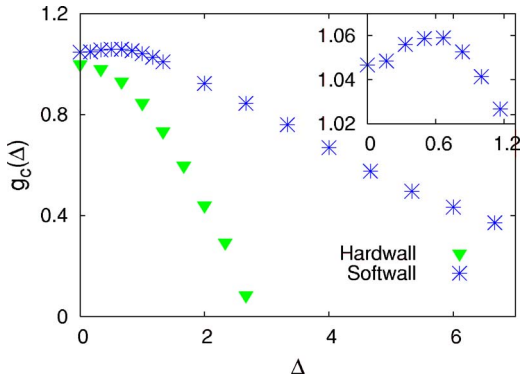

FIG. 4. (Color online) Critical force vs disorder strength for both the hard-wall and the soft-wall cases at $\beta\epsilon=15$, i.e. ($T=0.067$). The thin slice of reentrance is shown in the inset.

presented below. We show in Figs. 4 and 5 the final phase diagrams obtained by the same numerical procedure for the random system. These constitute a part of the major findings of this paper.

B. Units and dimensions

Throughout the paper we choose dimensionless quantities: Boltzmann constant k_B is chosen such that $\epsilon/k_B=1$, and in this unit, $k_B=1$ with temperature T as dimensionless. Distances are measured in units of lattice spacing $a=1$ (along the diagonal). The quantities like force (g), width (Δ), and potential V have dimension of energy and are measured in units of ϵ. All the plots shown in this paper use the dimensionless forms where $g\to g/\epsilon, T$ is $k_BT/\epsilon, V\to V/\epsilon, \Delta \to \Delta/\epsilon$, and $x\to x/a$. In case there is no adsorbtion energy, the relevant parameter is Δ/k_BT and the choice of ϵ does not matter.

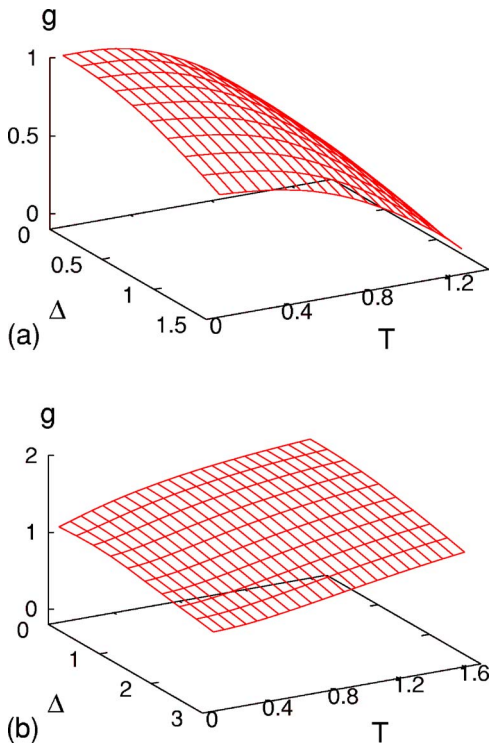

FIG. 5. (Color online) Phase surface for (a) hard-wall and (b) soft-wall in the presence of disorder.

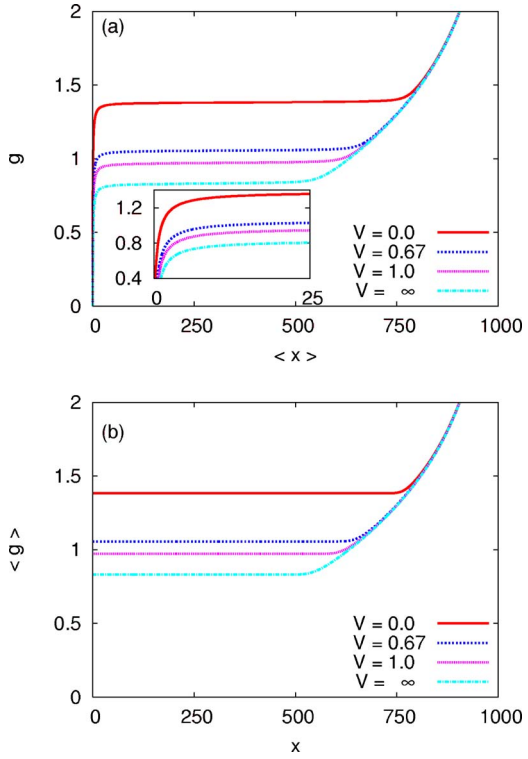

FIG. 6. (Color online) Force distance isotherms in (a) fixed force ensemble and (b) fixed distance ensemble, for a polymer of length $N=2000$ at $\beta\epsilon=1.5$ ($T=0.067$). Each lattice site on one side of the wall contains a repulsive potential of strength "V" and polymer is pulled away from the wall on the other side. The inset in (a) shows the knees which developed in the fixed force ensemble for low x but are absent in the fixed distance ensemble.

C. Isotherms

For the unzipping transition, $\langle x\rangle$ vs g or $\langle g\rangle$ vs x isotherms (depending on the ensemble) are of interest. The phase diagram can be mapped out from the special features of these isotherms. The procedure is explained for the pure case and the numerical results are compared with the exact results. This procedure is to be adopted for the random case.

Figure 6 shows the isotherms for the pure case. For finite N, these are obtained by iterating the recursion relation ("transfer matrix" approach) to calculate the partition function and then the extension or the force depending on the ensemble used. Except for a region near $x=0$, the two are identical (within numerical accuracy). The difference in the short distance region is expected because x in the fixed distance ensemble has to be an integer but $\langle x\rangle$ in the fixed force ensemble need not be [24].

The flat region in the g vs x isotherm signals a coexistence between a zipped and an unzipped (desorbed) phase. This is for a first order transition. The critical value $g_c(T)$ is obtained from the intersection of the flat part of the g-x isotherm with

the isotherm of the pure phases. For a higher order transition, there may not be any flat region but some singular feature would persist. In either case singularity on the isotherm gets rounded for finite N, and a finite size scaling analysis can be done to extract the critical value. The advantage of using this finite size scaling is that it does not rely on the order of the transition. This method remains valid even if there is no flat part of the isotherm (signaling a higher order transition). The exact solution suggests a scaling form for extensibility χ,

$$\chi = N^{d_\chi}\mathcal{X}((g-g_c)N^{\phi}) \tag{16}$$

with two characteristic exponents d_χ and ϕ. As we argue in Appendix A, the scaling variable for the pure problem is $N(g-g_c)$ so that $\phi=1$.

The scaling variable in Eq. (16) can be taken to imply that the length m of the unzipped region (see Fig. 2) depends on the force as a power law,

$$m \sim |g-g_c|^{-1/\phi}. \tag{17}$$

This length m has been used in studying the dynamics of unzipping of DNA [11].

If we demand extensivity for χ for $N\to\infty$, then $\mathcal{X}(x) \sim |x|^{-(d_\chi-1)/\phi}$. This implies

$$\chi/N \sim |g-g_c|^{-(d_\chi-1)/\phi}. \tag{18}$$

A similar scaling form can be written for the specific heat (per monomer). At a fixed force, the temperature dependence of the specific heat is

$$c_g(T) = N^{\alpha\phi_t}\mathcal{Y}([T-T_c(g)]N^{\phi_t}), \tag{19}$$

which defines the exponent ϕ_t in addition to the usual bulk specific heat exponent α. To recover the bulk behavior, $\mathcal{Y}(x)\sim|x|^{-\alpha}$ for large x. For a first order transition, $\alpha=1$.

The unzipping transition is characterized by the four exponents, $d_\chi, \phi, \alpha, \phi_t$. These are known from the exact solution and we compare them with the numerical results. These are also the quantities needed for the random system.

IV. TRANSFER MATRIX: NUMERICAL RESULTS FOR THE PURE CASE

We use the transfer matrix technique in both the ensembles to calculate the exact partition function numerically from the recursion relations in Eqs. (2) and (5).

In Fig. 7, an example of data collapse for extensibility χ for the hard-wall case is shown. This is at $\beta\epsilon=15(T=0.067)$ for $N=1000$, 1500, and 2000. The critical exponents suggested by collapse [22] are

$$d_\chi = 2, \quad \text{and } \phi = 1, \tag{20}$$

consistent with the exact solution in Appendix A. This implies

$$\chi/N \sim |g-g_c|^{-1}, \quad \text{and } m \sim |g-g_c|^{-1}. \tag{21}$$

In the thermodynamic limit, both the ensembles give the same phase boundary. By the data collapse method for the extensibility, the critical force $g_c(T)$ can be determined for a given T. Once the critical force is known, the size (N) dependence of the average distance $\langle x_i\rangle$ of the ith monomer for forces below and above it can be determined. We have checked that for g below g_c, $\langle x_i\rangle$ decreases very rapidly with N showing that the polymer is adsorbed on the wall whereas for g slightly above g_c the polymer is desorbed from the wall with $\langle x_i\rangle \propto i$.

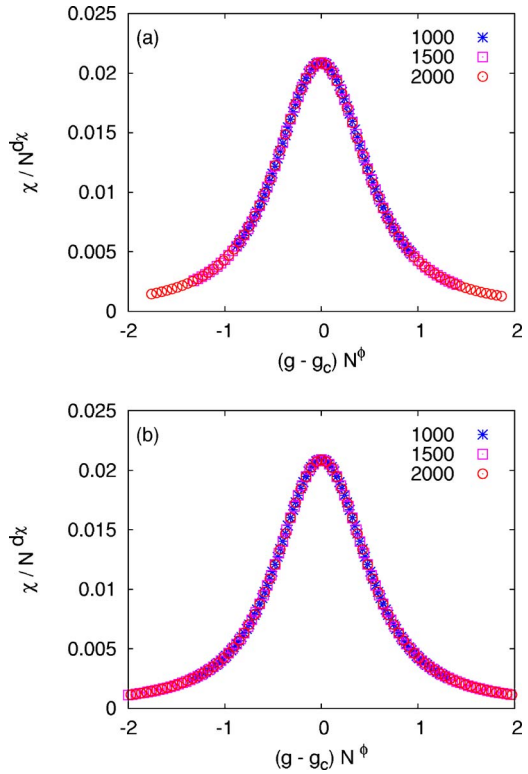

FIG. 7. (Color online) Data collapse of extensibility at $\beta\epsilon=15(T=0.067)$ for the pure case (a) soft-wall and (b) hard-wall. The lengths of the chain used are $N=1000$, 1500, and 2000. For both cases, the exponents are $d_\chi=2$ and $\phi=1$.

Also from the same calculation the specific heat has been computed. A comparison of the specific heat is shown in Fig. 8. The finite size scaling variable that one gets from the specific heat is of the form $[T-T_c(g)]N^{\phi_t}$ with $\phi_t=1$. Though a good collapse is obtained for $\alpha=0.93$, the error bar does not preclude $\alpha=1$ [shown in Fig. 8(b)], especially if there are finite corrections. The development of the δ-function peak ($\alpha=1$) at the transition point is a vindication of the first order nature of the unzipping transition.

The critical values obtained from data collapse of the numerical results are used to construct the phase diagram. These are shown in Fig. 3. The numerical results (points) are in good agreement with the analytical results (lines).

V. RANDOM CASE: PHASE DIAGRAM

To get the phase diagram we need to calculate the critical force, $g_c(T)$, at different disorder strengths and temperature keeping the binding to the wall constant. We use the finite size scaling of the correlation function for that purpose. For a disorder problem, depending on the way disorder averaging

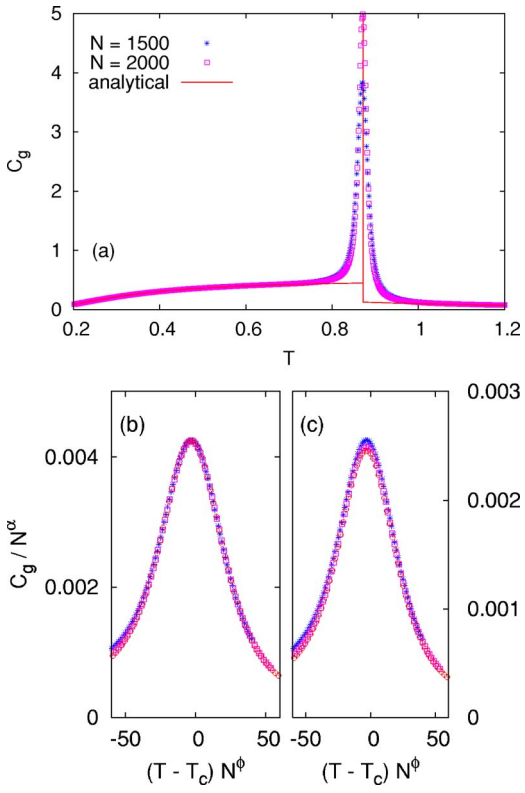

FIG. 8. (Color online) Specific heat up to a multiplicative constant for $g=1.0$. (a) There is a peak developing as N increases, over and above a discontinuity at $T_c(g)=0.872\,04$. (b), (c) Data collapse at $T_c(g)$ for chains of length $N=1500$, 2000, and 2500, with $\phi_t=1$ and $\alpha\phi_t=0.93$ in (b) but $\alpha\phi_t=1$ in (c).

is done, two different correlation functions can be defined.

$$\chi_{\rm dis} = \left[\langle x^2\rangle - \langle x\rangle^2\right]_{\rm dis} \tag{22a}$$

and

$$\mathcal{C}_{\rm dis} = \left[\langle x^2\rangle\right]_{\rm dis} - \left[\langle x\rangle\right]^2_{\rm dis}. \tag{22b}$$

For Eq. (22a) the disorder averaging is done at the response function level of an individual sample whereas for Eq. (22b), the disorder averaging is done at the moment level. The critical exponents for these two different correlation functions may not be the same. For the problem in hand, correlation functions scale as

$$\chi_{\rm dis} = N^{d_\chi}\mathcal{W}((g-g_c)N^{\phi}) \tag{23a}$$

and

$$\mathcal{C}_{\rm dis} = N^{d_\mathcal{C}}\mathcal{W}((g-g_c)N^{\phi}) \tag{23b}$$

where d_χ and $d_\mathcal{C}$ are the critical exponents for $\chi_{\rm dis}$ and $\mathcal{C}_{\rm dis}$, respectively, with ϕ describing the finite size behavior of the force. For the random problem, ϕ is expected to be different from the pure case of Eq. (16).

In the fixed distance ensemble the force, $g^{\{\alpha\}}(x,T)$, required to maintain a distance x from the wall is computed for each realization by taking the finite differences in free energy $F^{\{\alpha\}}(x,N)=-k_BT\log Z^{\{\alpha\}}(x,N)$, which on averaging over samples give the average force, $\langle g(x,T)\rangle$, required to maintain the distance x.

$$\langle g(x,T)\rangle = \left[F_N^{\{\alpha\}}(T,x+a) - F_N^{\{\alpha\}}(T,x)\right]_{\rm dis}/a, \tag{24}$$

where a is the lattice constant (in our case $a=1$). This has also been used to generate the phase diagram or cross-check the results.

The data collapse for both the correlation functions are shown in Fig. 9. The exponents for the hard-wall case, as suggested by the collapse, are

$$\phi = 0.5, \quad d_\chi = 1.5, \quad \text{and } d_\mathcal{C} = 2.0. \tag{25}$$

For both the correlation functions we obtain the same g_c value suggesting that any of them can be used to calculate the critical force. It is found that the correlation function at the moment level [Eq. (23b)] behaves more smoothly than the response function [Eq. (23a)] and so Eq. (23b) can be used to calculate g_c with the same accuracy for less number of realizations.

The phase diagram obtained by this determination of $g_c(T)$ for various T and the dimensionless disorder strength Δ is shown in Figs. 4 and 5. For small enough Δ and also small T, the random energies at the off-wall sites are not energetically favorable to delocalize the polymer. But still there are pockets or sites with locally favorable energies. The pulling force then has to pull the polymer out of the wall and the local pockets signaling an increase in the critical force until entropic effects start dominating or the disorder favors a delocalized state. Such a thin slice of reentrance for small Δ is shown in the inset in Fig. 4. The full three-dimensional surface in the $g-T-\Delta$ space is shown in Fig. 5 for the hard- and the soft-wall cases separately.

From the determined values of the exponents, we find that the quenched averaged extensibility χ, which has to be extensive, should have the same behavior as the pure case, namely,

$$\chi/N \sim |g-g_c|^{-1}, \quad \text{and } m \sim |g-g_c|^{-2}. \tag{26}$$

It is to be noted that for heterogeneous chain this extensibility has been predicted to be $|g-g_c|^{-2}$, though the finite size exponent ϕ is 1/2. In other words, the average behavior of the extensibility remains purelike though the size dependence or the scaling variable is like a heterogeneous chain case. This is one of the important conclusions of this paper. For a soft-wall case, as shown in Fig. 9, the exponents are the same as in the hard-wall case.

The zero force specific heat is shown in Fig. 10(a). Unlike the pure case, the discontinuity at the transition temperature is not clearly visible. It is interesting to note that all the specific heat curves for different values of N seem to cross at the same temperature. Such crossings generally imply existence of a certain "universal" scale [25]. In the present case this scale could be due to the proximity of the phase transition point but its identification remains to be done. There is a size dependence of the specific heat near the peak as N increases. This may be a signal of a very weak divergence of specific heat or even the formation of a cusp ($\alpha<0$). Figure

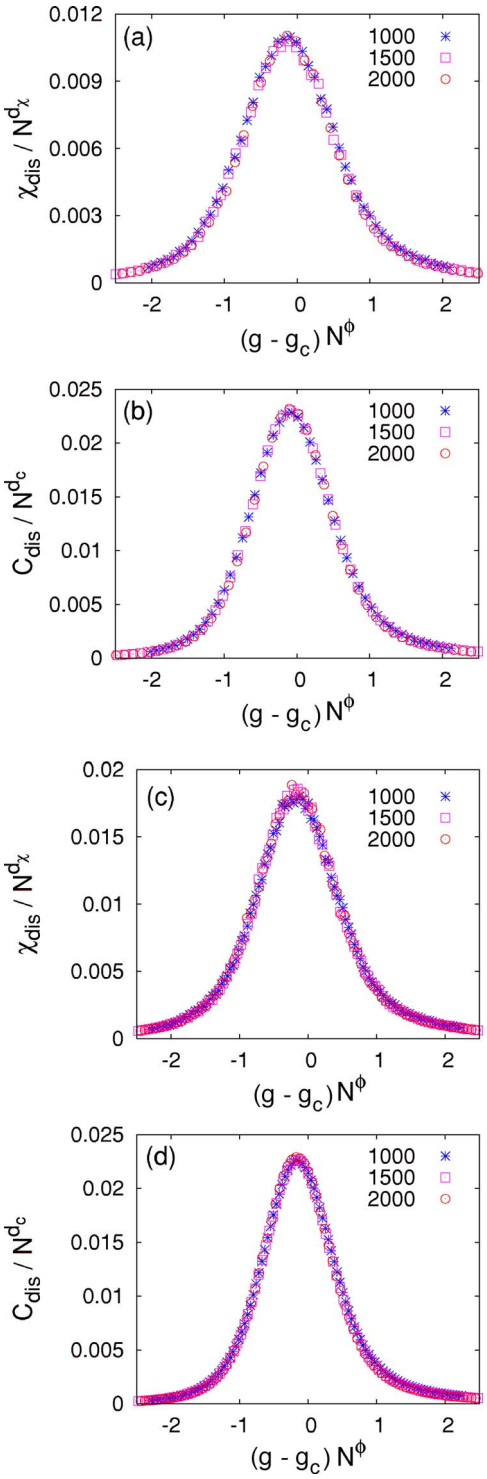

FIG. 9. (Color online) Data collapse for two different correlation functions for the random system. (a), (b) are for hard-wall and (c), (d) are for soft-wall. The chain length $N=1000$, 1500, and 2000. In (a) and (c) the disorder averaging is done at the response function level of an individual sample (by definition it is the extensibility up to a factor of T^{-1}). The exponents are $d_\chi=1.5, \phi=0.5$. In (b) and (d) averaging is done at moment level. The exponents are $d_C=2.0, \phi=0.5$. For all these correlation functions, the disorder strength $\Delta=2/3$ and averaging is done over 10^5 realizations at $\beta\epsilon=15(T=0.067)$.

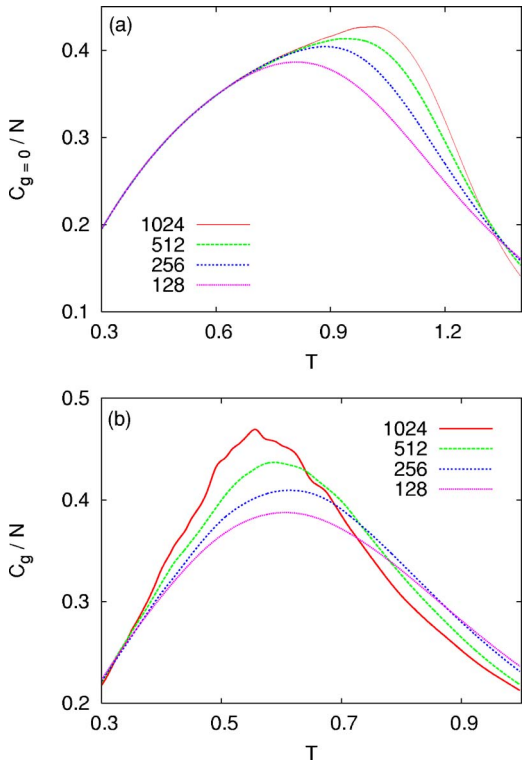

FIG. 10. (Color online) Specific heat for the random system at (a) $g=0$ and (b) $g=1$. There is a finite size dependence which, however, does not scale to yield a good data collapse. The averaging is done over 10^4 samples.

10(b) shows the specific heat vs T for $g=1.0$. Here also we see a growth in the peak, but it is not as sharp as in the pure case (Fig. 8). No good collapse can be obtained. Whether a delta peak is forming as $N\to\infty$ is not obvious. Longer chains need to be studied to sort out these issues.

VI. SAMPLE FLUCTUATIONS

A. Response

To study the response of the force, the partition function is computed for polymer of lengths up to $N=2048$ at a fixed temperature T, binding to the wall ϵ and disorder strength Δ. The average distance of the last monomer, X, where a fixed force g is applied (fixed force ensemble) is

$$X = \left[\langle x^{\{\alpha\}}\rangle\right]_{\text{dis}} = \left[\sum_x x P^{\{\alpha\}}(x)\right]_{\text{dis}} \tag{27}$$

where

$$P^{\{\alpha\}}(x) = \frac{Z_N^{\{\alpha\}}(x)}{\sum_x Z_N^{\{\alpha\}}(x)} \tag{28}$$

is the probability of the end monomer of sample α being at a distance x from the wall.

Figure 11 shows the rescaled force $gN^{1/3}$ versus rescaled separation $\langle x\rangle/N^{2/3}$ from the wall [Fig. 11(a)] and the extensibility [Fig. 11(b)] for four different samples of lengths $N=1024$ and $N=2048$ at $\beta\epsilon=15(T=0.067)$ for disorder

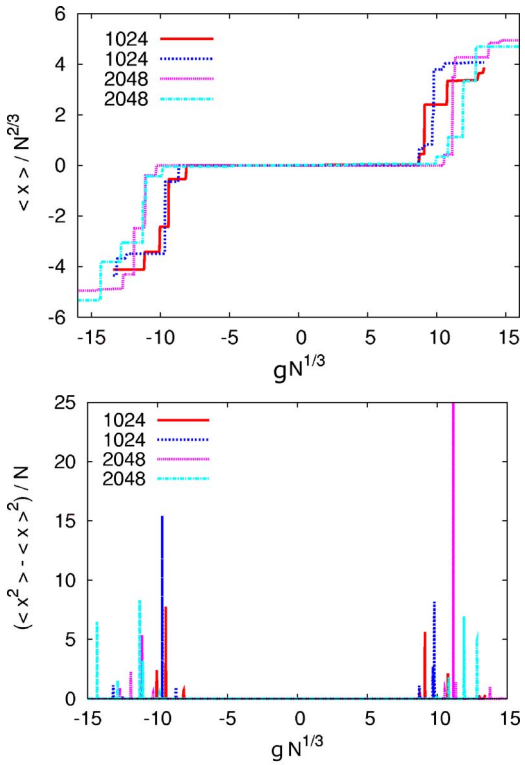

FIG. 11. (Color online) (a) Rescaled force $gN^{1/3}$ vs rescaled average distance $\langle x\rangle/N^{2/3}$, from the wall for four different samples of size $N=1024$ and $N=2048$ at $\beta\epsilon=15(T=0.067)$ for the disorder strength $\Delta=2$ when there is binding to the wall. (b) Extensibility for the same samples.

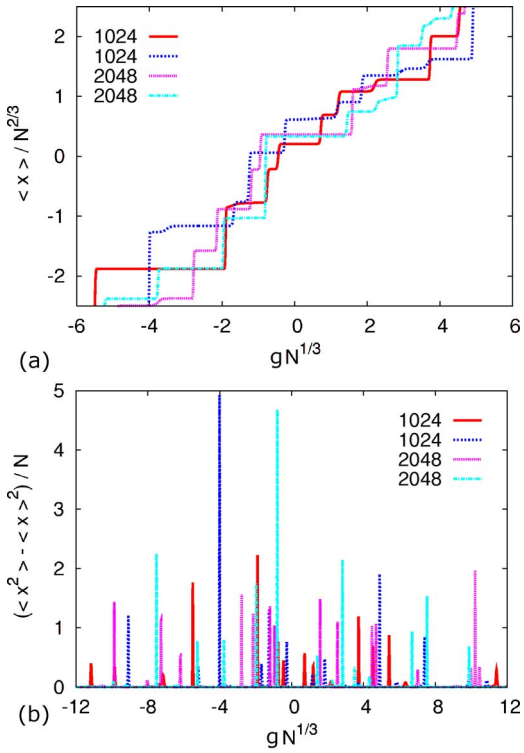

FIG. 12. (Color online) (a) Rescaled force $gN^{1/3}$ vs rescaled average distance $\langle x\rangle/N^{2/3}$ from the wall for four different samples of size $N=1024$ and $N=2048$ at $\beta\epsilon=15(T=0.067)$ for the disorder strength $\Delta=2$ and there is no binding to the wall ($\epsilon=0$). (b) Extensibility for the same samples.

strength $\Delta=2$ when there is a soft-wall. The large plateau for small force shows that the energy gain from the wall favors the adsorption of polymer and some critical force, which depends on sample, is needed to desorb it. Above this critical force the polymer does not see the wall but because of the randomness it can still get trapped in some attractive sites. The distance from the wall does not increase when the force is increased by a small amount. The response would then just be the thermal width of the probability distribution which at low temperatures is very narrow and independent of N. As a result small plateaus develop in the isotherm for any specific sample as shown in the plot [21,26]; but because of the possibility of nearly degenerate but spatially separated states, a fixed force of the right amount may produce a large displacement. Consequently, sharp jumps appear between plateaus in the isotherms. The corresponding extensibility of a sample shows spikes (delta function peaks) where there are jumps in the force versus distance curves and it is zero within plateaus. Note the ensemble difference here. Whereas a small change in g (in the fixed force ensemble) can produce a large change in x, in the fixed distance ensemble, a small change in x would just explore the neighborhood of the preferred configuration. The spikes of Fig. 11(b) remain undetected. On averaging over samples, we need to get back extensivity for the extensibility χ. This is possible because of rare samples with probability $\sim N^{-2\nu+1}$ having degenerate but spatially separated states (allowing unzipping at zero-force) [21].

The plot between rescaled force and rescaled distance from the wall and the corresponding extensibility, but with $\epsilon=0$, for the same parameters is shown in Fig. 12. The average response of the force is linear at small forces [26].

It is interesting to calculate the probability distribution for average height of steps, Δx. Figure 13 shows a log-log plot of $P(\Delta x)$ versus the step height Δx. Here we have assumed that the steps are independently distributed. These are taken

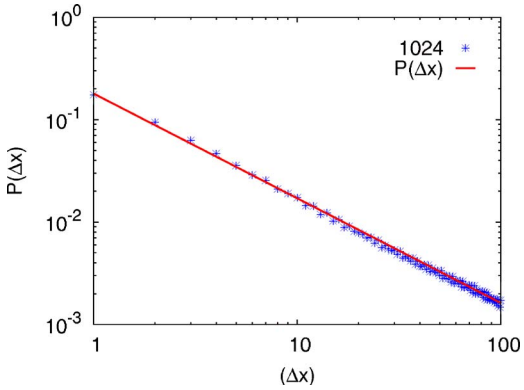

FIG. 13. (Color online) Log-log plot of the probability distribution $P(\langle\Delta x\rangle)$ of the rescaled average step height $\langle\Delta x\rangle$. This is for a polymer of length $N=1024$ in a fixed force ensemble at $\beta\epsilon=15(T=0.067)$, disorder strength $\Delta=2$, and there is no binding to the wall ($\epsilon=0$). 10^5 samples are used to generate the statistics. The slope of the fitted line is 1.

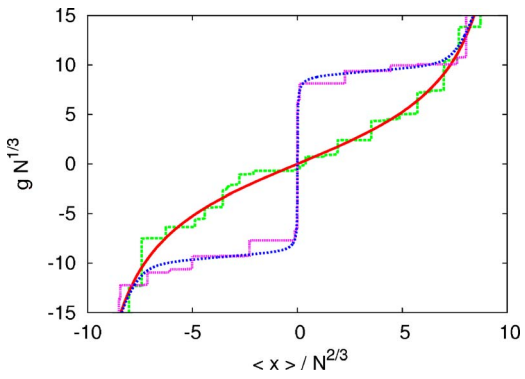

FIG. 14. (Color online) Rescaled force $gN^{1/3}$ vs rescaled average distance $\langle x\rangle/N^{2/3}$, from the wall for a polymer of length $N=2048$ at $\beta\epsilon=15(T=0.067)$. The disorder is kept the same (at a disorder strength $\Delta=2$) for both binding and no binding ($\epsilon=0$) to the wall. The steps are for a single sample and smooth curves are after averaging over 10^4 samples.

over 10^5 samples at $\beta\epsilon=15(T=0.067)$ and disorder strength $\Delta=2$. The straight line is the best fit which suggests the probability distribution of the form

$$P(\Delta x) \sim (\Delta x)^{-p} \tag{29}$$

with $p=1$.

In Fig. 14 we have plotted again the rescaled separation with rescaled force for both binding and no binding to the wall but by keeping the underlying disorder the same at a disorder strength ($\Delta=2$) and $\beta\epsilon=15(T=0.067)$ for $N=1024$. The steps are for a single sample and the smooth curves are for averages over 10^4 samples. For large values of force both the curves merge showing that the effect of the binding is negligible at large force.

B. Pseudocritical force

It is clear from Fig. 11 that in the random environment, the critical force needed to unzip a polymer depends strongly on sample. For example, the displacement for a particular sample would depend on the deviation $g-g_0$, where g_0 is the critical force for that sample. A random system may have another scale that shows the closeness of g_0 to the average critical force g_c. The scaling behavior of this scale can be obtained from the probability distribution of g_0 or the finite size scaling of the distribution, $P(g_0)=N^{d_g}\mathcal{F}(|g_0-g_c|N^{\phi_g})$ that defines d_g and ϕ_g.

We take the first jump from the wide plateau around $g=0$ as the measure of the (pseudo) critical force, g_0. The scaled probability distribution obtained from the frequencies of g_0 over 10^5 samples for $N=512$ and 1024 is shown in Fig. 15. The plot suggests $d_g=0.41$ and $\phi_g=0.31$, which also implies a sharply peaked probability distribution. The fact that $\phi_g \neq \phi$ (see Fig. 9) is suggestive of different scaling of the two different scales.

C. Bubble, spacer, and unzipped segments

In the random medium, the disorder controls the configuration of the polymer. As already said, the critical force needed to unzip the polymer is sample dependent. It is interesting to study the distribution of various quantities such as bubble length, length of adsorbed or zipped and desorbed or unzipped segments with the applied force.

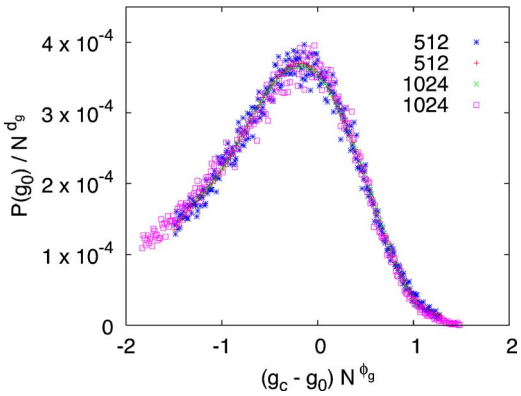

FIG. 15. (Color online) Data collapse for the probability distribution of pseudocritical force $P(g_0)/N^{d_g}$ vs $(g_c-g_0)\hat{N}^{\phi_g}$ for the hard-wall case for $N=512$ and 1024. $d_g=0.41$ and $\phi_g=0.31$. The averaging is done over 10^5 samples.

Figure 16 shows the average separation from the hard-wall for each monomer of chain of length $N=300$ at a temperature $\beta\epsilon=3(T=1/3)$ and disorder strength $\Delta=5/3$ when a stretching force $g=0.5$ is applied at the end. Four different chain configurations are shown by the dotted and dashed lines whereas the curve with solid line is the result of averaging over 90 000 such chain configurations. Although the applied force here is below the critical force needed to desorb the polymer; there are some samples which are in the desorbed phase.

In this paper we concentrate only on the probability distribution of (i) the length of the desorbed or unzipped segment, (ii) the length of the adsorbed or zipped segment between unzipped segment and the bubble (spacer), and (iii) the length of the first bubble. These quantities are defined schematically in Fig. 2.

The probability distribution (over samples) for the unzipped length $P(m)$, for the length m of the chain which gets

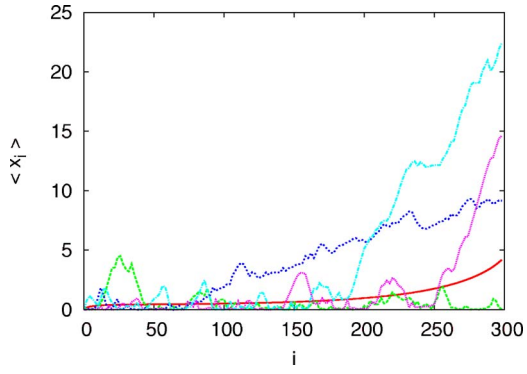

FIG. 16. (Color online) Average separation from the wall, $\langle x_i\rangle$, of ith monomer of chain of length $N=300$ at $\beta\epsilon=3(T=1/3)$ and disorder strength $\Delta=5/3$ when a stretching force $g=0.5$ is applied at one end. Four different chain configurations are shown by the dotted and dashed lines. The solid line is when averaging is done over 90 000 samples.

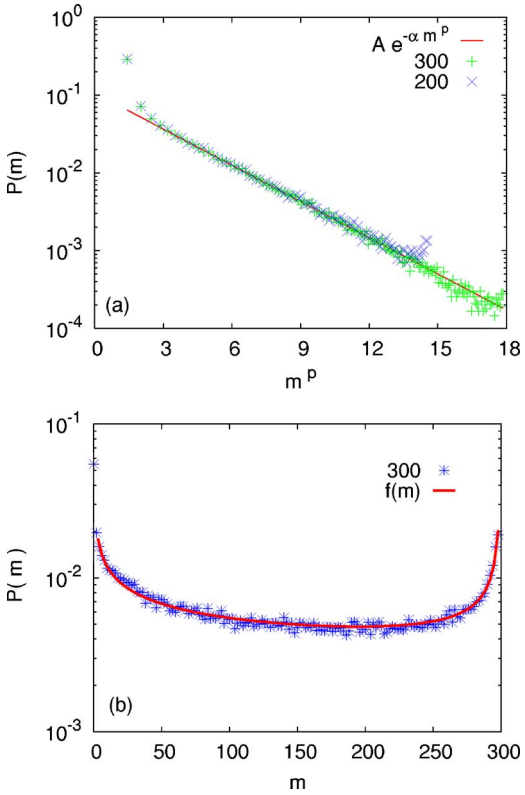

FIG. 17. (Color online) Probability distribution of the unzipped length m. (a) Plot of $P(m)$ vs m^p, at $\beta\epsilon=3\,(T=0.333)$ and disorder strength $\Delta=5/3$, when a stretching force $g=0.5$ is applied at the end. The points are for $N=200$ and 300 and the solid line is the fit using the functional form $f(m)=Ae^{-\alpha m^p}$. Here $p=0.51\pm0.01$. (b) Plot of $P(m)$ vs m at $\beta\epsilon=3\,(T=1/3)$, a force $g=g_c=0.82$ is applied. This is the force on the phase boundary. The solid curve is the fit using the functional form $f(m)=c_0/m^{b_0}+c_1/(N-m)^{b_1}$. To obtain the fit, we have excluded $m=0$ and $m=N$. For this plot $c_0=0.026\pm0.001, b_0=0.37\pm0.01, c_1=0.028\pm0.001$, and $b_1=0.71\pm0.02$ are the fitting parameters. $N=300$ for both the figures.

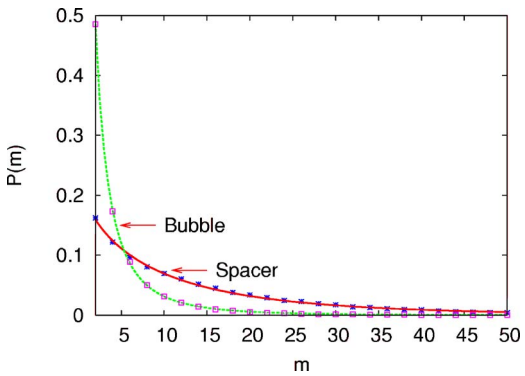

FIG. 18. (Color online) Probability distribution of length of the spacer, and the length of the first bubble, at critical force $g_c=0.82$ and $\beta\epsilon=3\,(T=1/3)$ for a disorder strength $\Delta=5/3$. A fitting function of the form $f(m)=Ae^{-\alpha m^c}$ is used to fit the data. The best fit gives the value $c=0.72\pm0.01$ for zipped segment and $c=0.31\pm0.01$ for the first bubble.

desorbed or unzipped at the phase boundary is shown in Fig. 17. For force below the phase boundary, the probability distribution decays rapidly with length [Fig. 17(a)] but not so on the phase boundary [Fig. 17(b)]. For $g<g_c(T)$, the probability distribution seems to be stretched-exponential, $P(m)\sim\exp(-a\sqrt{m})$, but the distribution for the phase boundary seems to admit power laws, especially near the peaks at the two extremes. Such a two peak structure is expected at a phase coexistence.

Figure 18 shows the probability distributions for the length of spacer (m_s) and the length of the first bubble (m_b). Both the distributions at phase boundary are stretched-exponential $P(m_s)\sim\exp(-am_s^{c_s})$ with $c_s=0.72\pm0.01$ for spacer length and $P(m_b)\sim\exp(-am_b^{c_b})$ with $c_b=0.31\pm0.01$ for the bubble.

VII. SUMMARY

We obtained the exact phase boundary of unzipping of a polymer in 1+1 dimensions from a wall separating two regions of different affinity for the polymer. We developed a procedure to generate the phase diagram from an exact numerical procedure and for the pure case the numerical results do reproduce the exact results. The unzipping transition is characterized by a set of exponents describing the length dependence of the extensibility and the specific heat. Numerical results on the exponents also agree with the exact results, namely $d_\chi=2, \phi=1, d_C=1$, and $\phi_t=1$.

In the presence of random impurities distributed independently, taken from uniform deviate of width Δ, a free polymer wanders more than in a pure medium. In addition there is a free energy fluctuation that grows with the length. It is natural that there is a sample dependence of the unzipping process but the response under large force also has an inner structure characteristic of the local pockets of favorable sites. However, the steps one sees in the response averages out and one gets a smooth quenched averaged isotherm. The phase diagram is determined both for a hard-wall and a soft-wall. The exponents $d_\chi=1.5, \phi=0.5$ are different from the pure. The behavior of the specific heat and finer details of the sample dependence need further studies. Probability distributions of various relevant quantities are also obtained.

APPENDIX A: PHASE BOUNDARY FOR PURE CASE

In this Appendix we give details to calculate the phase boundary for a pure problem. As stated earlier, we consider a more general case by assuming that there is a potential $V(V>0)$ at each lattice site on one side of the wall. The soft-wall and hard-wall are then the limiting cases for $V\to0$ and $V\to\infty$, respectively, of the problem. The recursion relation satisfied by the canonical partition function in the presence of potential is

$$Z_{N+1}(x)=\begin{cases}[Z_N(x+1)+Z_N(x-1)]e^{-\beta V} & \text{for } x<0\\ Z_N(x+1)+Z_N(x-1) & \text{for } x>0\\ [Z_N(+1)+Z_N(-1)]e^{\beta\epsilon} & \text{for } x=0\end{cases} \tag{A1}$$

with the initial condition $Z_0(x)=e^{\beta\epsilon}\delta_{x,0}$. The generating function for the partition function,

$$G(z,x) = \sum_N z^N Z_N(x), \tag{A2}$$

can be taken to be of the form (ansatz)

$$G(z,x) = \begin{cases} \lambda^x A & \text{for } x > 0 \\ \lambda'^{-x} A & \text{for } x < 0 \end{cases} \tag{A3}$$

with λ, λ', and A to be determined (z dependence of λ, λ' suppressed). The root test of convergence then tells us that the singularity closest to origin (on the positive real axis) in the complex z-plane determines the partition function for $N \to \infty$. For finite N, a contour integration with deformation around the singularities of $G(z,x)$ in the z-plane would yield Z_N from Eqs. (A2) and (A3).

Using the ansatz Eq. (A3) in Eq. (A2), we get

$$\frac{\lambda'}{z} = [\lambda'^{-x-1} + \lambda'^{-x+1}] e^{-\beta V} \quad \text{for } x < 0, \tag{A4a}$$

$$\frac{\lambda^x}{z} = [\lambda^{x+1} + \lambda^{x-1}] \quad \text{for } x > 0, \tag{A4b}$$

$$\frac{A}{z} = \left[(\lambda' + \lambda) A + \frac{1}{z} \right] e^{\beta\epsilon} \quad \text{for } x = 0, \tag{A4c}$$

from which one obtains

$$\lambda = \frac{1 - \sqrt{1 - 4z^2}}{2z}, \tag{A5a}$$

$$\lambda' = \frac{1 - \sqrt{1 - 4z^2 e^{-2\beta V}}}{2z e^{-\beta V}}, \tag{A5b}$$

and

$$A = \frac{1}{1 - (\lambda' + \lambda) z e^{\beta\epsilon}}. \tag{A5c}$$

The singularities coming from λ and λ' are

$$z_1 = \frac{1}{2}, \quad \text{and } z_1' = \frac{1}{2 \exp(-\beta V)}. \tag{A6}$$

A has the singularity

$$z_2 = \frac{1}{2} \sqrt{1 - \left(1 - \frac{2e^{-\beta\epsilon}(1 - e^{-\beta V} e^{-\beta\epsilon})}{1 + e^{-\beta V}(1 - 2e^{-\beta\epsilon})} \right)^2}, \tag{A7}$$

which depends on both the adsorption energy and the potential V. On taking the limit $V \to 0$, the problem reduces to the soft-wall case. On the other hand the problem reduces to a hard-wall case in the limit $V \to \infty$. In these limits z_2 becomes

$$z_2 = \begin{cases} \frac{1}{2} \sqrt{1 - (1 - e^{-\beta\epsilon})^2} & \text{for soft-wall} \\ \frac{1}{2} \sqrt{1 - (1 - 2e^{-\beta\epsilon})^2} & \text{for hard-wall.} \end{cases} \tag{A8}$$

The relevant partition function in fixed distance ensemble for large N is approximated by

$$Z_N(x) \sim \frac{\lambda^x(z_2)}{z_2^{N+1}} \text{ for } x > 0, \tag{A9}$$

via the contour integration method, with z_2 as the closest-to-origin singularity. The free energy is then

$$\beta F(x) = N \ln z_2 - x \ln \lambda(z_2), \tag{A10}$$

up to x-independent additive constant. The force required to maintain the distance x is given by $g = 2 \partial F / \partial x$. A factor of 2 is needed as per our definition of unit length as the diagonal of a unit square of Fig. 1. The phase boundary is then given by

$$g_c(T) = -2T \ln \lambda(z_2), \tag{A11a}$$

or

$$g_c(T) = T \ln \left[\frac{1 + e^{-\beta V}(1 - 2e^{-\beta\epsilon})}{e^{-\beta\epsilon}(1 - e^{-\beta V} e^{-\beta\epsilon})} - 1 \right], \tag{A11b}$$

which has been quoted in Eq. (14a). On taking the limit $V \to 0$ and $V \to \infty$ one gets, respectively, the phase boundary for soft-wall and hard-wall.

$$g_c(T) = \begin{cases} T \ln[2e^{\beta\epsilon} - 1] & \text{for soft-wall} \\ T \ln[e^{\beta\epsilon} - 1] & \text{for hard-wall.} \end{cases} \tag{A12}$$

The zero force melting takes place at $T_c = \infty$ for soft-wall and $T_c = \epsilon / \ln 2$ for the hard-wall case. There is a nonzero T_c for any $V < \infty$.

In the fixed force ensemble, apart from above-mentioned singularities, an additional force dependent singularity, $z_3(\beta g) = [2 \cosh(\beta g)]^{-1}$, comes from the generating function (grand partition function)

$$\mathcal{G}(z, \beta g) = \sum_{N=0}^{\infty} z^N \sum_x Z_N(x) e^{\beta g x}. \tag{A13}$$

The phase boundary in the fixed force ensemble comes from equating two singularities $z_2 = z_3$. It is

$$g_c(T) = 2T \cosh^{-1} \left[\left\{ 1 - \left(1 - \frac{2u(1 - vu)}{1 + v(1 - 2u)} \right)^2 \right\}^{-1/2} \right] \tag{A14a}$$

with

$$u = e^{-\beta\epsilon}, \quad \text{and } v = e^{-\beta V}. \tag{A14b}$$

On taking the appropriate limits and with a little simplification, one gets

$$g_c(T) = \begin{cases} 2T \tanh^{-1}[1 - e^{-\beta\epsilon}] & \text{for soft-wall} \\ 2T \tanh^{-1}[1 - 2e^{-\beta\epsilon}] & \text{for hard-wall.} \end{cases} \tag{A14c}$$

With some algebra one can check that Eqs. (A12) and (A14c) are identical.

On pulling the polymer on the wrong side ($x < 0$, i.e., against the potential V), the phase diagram modifies as follows: In the fixed distance ensemble, the relevant free energy comes from the partition function $Z_N(x) \sim \lambda'^{-x}(z_2) / z_2^{N+1}$ which gives the phase boundary

$$g_c(T) = 2T \ln \lambda'(z_2). \tag{A15}$$

In the fixed force ensemble the force dependent singularity, $z_3(\beta g)$, of the generating function [Eq. (A13)] modifies to $z_3'(\beta g)=[2v\cosh(\beta g)]^{-1}$ which on equating with temperature dependent singularity, $z_2(\beta\epsilon)$ gives

$$g_c(T) = -2T\cosh^{-1}\left[\frac{1}{v}\left\{1-\left(1-\frac{2u(1-vu)}{1+v(1-2u)}\right)^2\right\}^{-1/2}\right]. \tag{A16}$$

The low temperature behavior of the phase boundary can be understood by a simple analysis. Since the wall is at $x=0$, only the even monomers can be on the wall. For the soft-wall case, this means the ground state has a degeneracy of 2^N for $2N$ steps because both sides of the wall are equally allowed. For small enough T, when a length $2m$ is stretched out by the force, the net change in the free energy would involve the loss of the bound state entropy and the gain in the energy due to stretching [10,11]. This give $F(m)=m\epsilon - gm + Tm\ln 2$, from which the low temperature phase boundary comes out as $g_c(T)=\epsilon+T\ln 2$.

For any $V>0$, the degeneracy is completely lifted as it is energetically not favorable to be on the negative x side of the wall. Consequently, there is no extra loss of entropy of the bound state at low temperatures. This explains the difference in the low temperature behavior of the phase boundary betweeen the soft-wall and the hard-wall case (including $V>0$).

Finite size behavior

Let us use the ansatz of Eq. (A3) in Eq. (A13), for finite N, the sum over x goes from $-N$ to N. Therefore we shall have terms of the type $[\lambda(z_2)e^{\beta g}]^N$ where Eq. (A9) has been used. Noting that the critical force is given by Eq. (A11a), the N dependent term (that vanishes for $N\to\infty$) is $e^{N\beta(g-g_c)}$. One can then identify the finite size scaling variable as $N(g-g_c)$ as quoted in Eq. (16).

APPENDIX B: SPECIFIC HEAT FOR THE PURE PROBLEM

For a given force g, the temperature, $T_c(g)$, at which the transition from the adsorbed to the desorbed phase takes place can be calculated by using Eq. (A12). Below $T_c(g)$ the polymer is adsorbed on the wall and the thermodynamic properties come from the free energy containing the binding term. The relevant partition function comes from z_2 of Eq. (A8). For the hard-wall case, the corresponding free energy is $N^{-1}\mathcal{F}(T,g)=T\ln z_2(T)$. The specific heat, which is the second derivative of the free energy is

$$C(T) = T\frac{d^2\mathcal{F}(T,g)}{dT^2} = \frac{\epsilon^2\exp(\epsilon/T)}{2T^2[\exp(\epsilon/T)-1]^2}. \tag{B1}$$

When the temperature exceeds $T_c(g)$ the polymer gets desorbed. In this case the thermodynamics is governed by the force dependent free energy $N^{-1}\mathcal{F}(T,g)=T\ln z_3$ where $z_3=1/[2\cosh(g/T)]$ is the force dependent singularity. Therefore the fixed-force specific heat is

$$C_g(T) = T\frac{d^2\mathcal{F}(T,g)}{dT^2} = \frac{g^2\,\mathrm{sech}^2(g/T)}{T^2}. \tag{B2}$$

There is a discontinuity at $T_c(g)$ but superposed on that there is a delta function for $g\neq 0$. A delta function at $T_c(g)$ shows that the transition is first order for $g\neq 0$. In the absence of force ($g=0$), only the discontinuity survives and it is then a classical second order phase transition.

[1] R. J. Rubin, J. Chem. Phys. **43**, 2392 (1966).
[2] V. Privman, G. Forgacs, and H. L. Frisch, Phys. Rev. B **37**, R9897 (1988).
[3] A. R. Veal, J. M. Yeomans, and G. Jug, J. Phys. A **23**, L109 (1990).
[4] Sumedha, J. Phys. A **37**, 3673 (2004).
[5] R. Rajesh, D. Dhar, D. Giri, S. Kumar, and Y. Singh, Phys. Rev. E **65**, 056124 (2002).
[6] A. Ashkin, Proc. Natl. Acad. Sci. U.S.A. **94**, 4853 (1997).
[7] B. Essevaz-Roulet, U. Bockelmann, and F. Heslot, Proc. Natl. Acad. Sci. U.S.A. **94**, 11935 (1997); U. Bockelmann, B. Essevaz-Roulet, and F. Heslot, Phys. Rev. E **58**, 2386 (1998).
[8] S. M. Bhattacharjee, e-print isskey cond-mat/9912297; J. Phys. A **33**, L423 (2000).
[9] K. L. Sebastian, Phys. Rev. E **62**, 1128 (2000).
[10] D. Marenduzzo, A. Trovato, and A. Maritan, Phys. Rev. E **64**, 031901 (2001).
[11] D. Marenduzzo, S. M. Bhattacharjee, A. Maritan, E. Orlandini, and F. Seno, Phys. Rev. Lett. **88**, 028102 (2002).
[12] Alexei V. Tkachenko, Phys. Rev. E **70**, 051901 (2004); Jeff Z. Y. Chen, *ibid.* **66**, 031912 (2002); D. K. Lubensky and D. R. Nelson, *ibid.* **65**, 031917 (2002), and references therein.
[13] R. Kapri, S. M. Bhattacharjee, and F. Seno, Phys. Rev. Lett. **93**, 248102 (2004).
[14] S. Kumar, D. Giri, and S. M. Bhattacharjee, Phys. Rev. E **71**, 051804 (2005).
[15] C. Danilowicz, Y. Kafri, R. S. Conroy, V. W. Coljee, J. Weeks, and M. Prentiss, Phys. Rev. Lett. **93**, 078101 (2004).
[16] E. Orlandini, M. C. Tesi, and S. G. Whittington, J. Phys. A **37**, 1535 (2004).
[17] P. K. Mishra, S. Kumar, and Y. Singh, Europhys. Lett. **69**, 102 (2005).
[18] L. Balents and M. Kardar, Phys. Rev. B **49**, 13030 (1994).
[19] T. Hwa and T. Nattermann, Phys. Rev. B **51**, 455 (1995).
[20] J. Wuttke and R. Lipowsky, Phys. Rev. B **44**, 13042 (1991).
[21] S. M. Bhattacharjee, e-print isskey cond-mat/0505283, *Statistics of Linear Polymers in Disordered Media*, edited by B. K. Chakrabarti (Elsevier, Amsterdam, 2005).

[22] S. M. Bhattacharjee and F. Seno, J. Phys. A **34**, 6375 (2001).
[23] In the context of vortex lines, the attracting line is often called a columnar pin. G. Blatter *et al.*, Rev. Mod. Phys. **66**, 1125 (1994).
[24] The situation is similar to the problem of chemical potential for small systems for which the number of particles is a small integer. See, e.g., T. A. Kaplan, e-print isskey cond-mat/0408103.
[25] S. G. Mishra and P. A. Sreeram, Eur. Phys. J. B **14**, 287 (2000).
[26] M. Mezard, J. Phys. (France) **51**, 1831 (1990).